Supporting Information

Carbazole-based D-A Type Hole Transport Materials to Enhance Performance of Perovskite Solar Cells

Haitao Liu,[a,b§] Bizu He,[b§] Huiqiang Lu,[b] Rong Tang,[b] Fei Wu*[b], Cheng Zhong,[c] Shufang Li,[b] Jinliang Wang,*[a] Linna Zhu*[b]

[a]Institute of Chemistry, Henan Academy of Sciences, Zhengzhou 450002, P. R. China.

E-mail: *jinliangw@hotmail.com*

[b]School of Materials & Energy, Southwest University, Chongqing 400715, P. R. China.

E-mail: *lnzhu@swu.edu.cn*; *feiwu610@swu.edu.cn.*

[c]Department of Chemistry, Wuhan University, Wuhan 430072, P. R. China.

1. General information

Materials and Instruments

Unless otherwisely stated, all starting materials were purchased from commercial suppliers (Sigma Aldrich, and the Energy Chemical) and used without further purification. Solvent for chemical synthesis such as toluene was freshly distilled over Na-K alloy under argon atmosphere prior to use. The nuclear magnetic resonance (NMR) spectra were obtained from a BRUKER AVANCE Ⅲ 600 MHz NMR Instrument(in $CDCl_3$ and THF-d_8). UV-vis absorption spectra were measured on a Shimadzu UV-2450 absorption spectrophotometer. Cyclic voltammetry (CV) tests were performed on a CHI-660A in CH_2Cl_2 under a nitrogen atmosphere, using saturated calomel electrode (SCE) as reference electrode and ferrocene as internal standard. Thermal gravimetric analysis (TGA) was

performed on a TGA Q50 at a heating rate of 10 °C min^{-1} under a nitrogen atmosphere. Differential scanning calorimetry (DSC) measurement was performed on a DSC Q20 instrument at a heating rate of 10 °C min^{-1} under a nitrogen atmosphere. Steady-state PL spectra were recorded on Fluorolog®-3 fluorescence spectrometer (Horiba). Atomic force microscopy (AFM) was used for characterizing the morphology using a CSPM5500 Scanning Probe Microscope (tapping mode). FE-SEM images were taken on JSM-7800F.

2. Device fabrication and testing

Preparation of HTM Solutions

As for the reference, the spiro-OMeTAD solution (72.5 mg sprio-OMeTAD, 28.5 μL 4-tertbutylpyridine (*t*-BP)) and 17.5 μL lithium-bis(trifluoromethanesulfonyl)imide (Li-TFSI) stock solution (520 mg mL^{-1} in acetonitrile) in 1 mL chlorobenzene were prepared according to literature.[1] Different HTMs (KZ, KZIC and KZRD) were all dissolved in CB in a concentration of 50 mg mL^{-1} , with *t*-BP and Li-TFSI as dopants.

Device fabrication

FTO-coated glass with sheet resistance of 14 Ω sq^{-1} were cleaned sequentially in deionized water, ethanol and acetone before undergoing 2 minutes of O_2 plasma treatment. The titanium precursor (350 μL titanium isopropoxide and 25 μL HCl in 5 mL isopropanol) was spin-coated on an FTO substrate at 5000 rpm for 60 s, and then calcined on a hot plate at 500 °C for 60 min (275 °C for 5 min, 325 °C for 5 min, 375 °C for 5 min, and 500 °C for 60 min) to deposit a compact layer of TiO_2. Subsequently, the mixed halide perovskite lead precursor (the mole ratio of PbI_2: $PbCl_2$: MAI is 1:1:4, 202.8 mg PbI_2, 122.7 mg $PbCl_2$ and 279.8 mg MAI in 1 mL DMF) was sequentially spin-coated on the substrate at 2000 rpm for 60 s, and then annealed at 100ºC for 45 minutes in a nitrogen-

filled glove box. The HTM solution was spin-coated onto the perovskite layer at 5000 rpm for 60 s. After oxidizing the HTM layer in air for 18 hours, the device was pumped to less than 10^{-5} torr, and then Ag counter electrode of about 100 nm thickness was deposited on top. The active area of our device is 0.06 cm^2.

SCLC measurements:

Hole mobility tests were conducted using a diode configuration of ITO/PEDOT:PSS/HTM/MoO_3/Ag by taking current-voltage in the range of 0-6 V and fitting the results to a space charge limited form, based on the following equation $J = 9\varepsilon_\theta\varepsilon_\gamma\mu_h V^2/8L^3$. J is the current density, L is the film thickness of the active layer, μ_h is the hole mobility, ε_γ is the relative dielectric constant of the transport medium ' ε_θ is the permittivity of free space ($8.85*10^{-12}$ F m^{-1}), V is the internal voltage of the device.

3. Synthetic procedures and characterizations

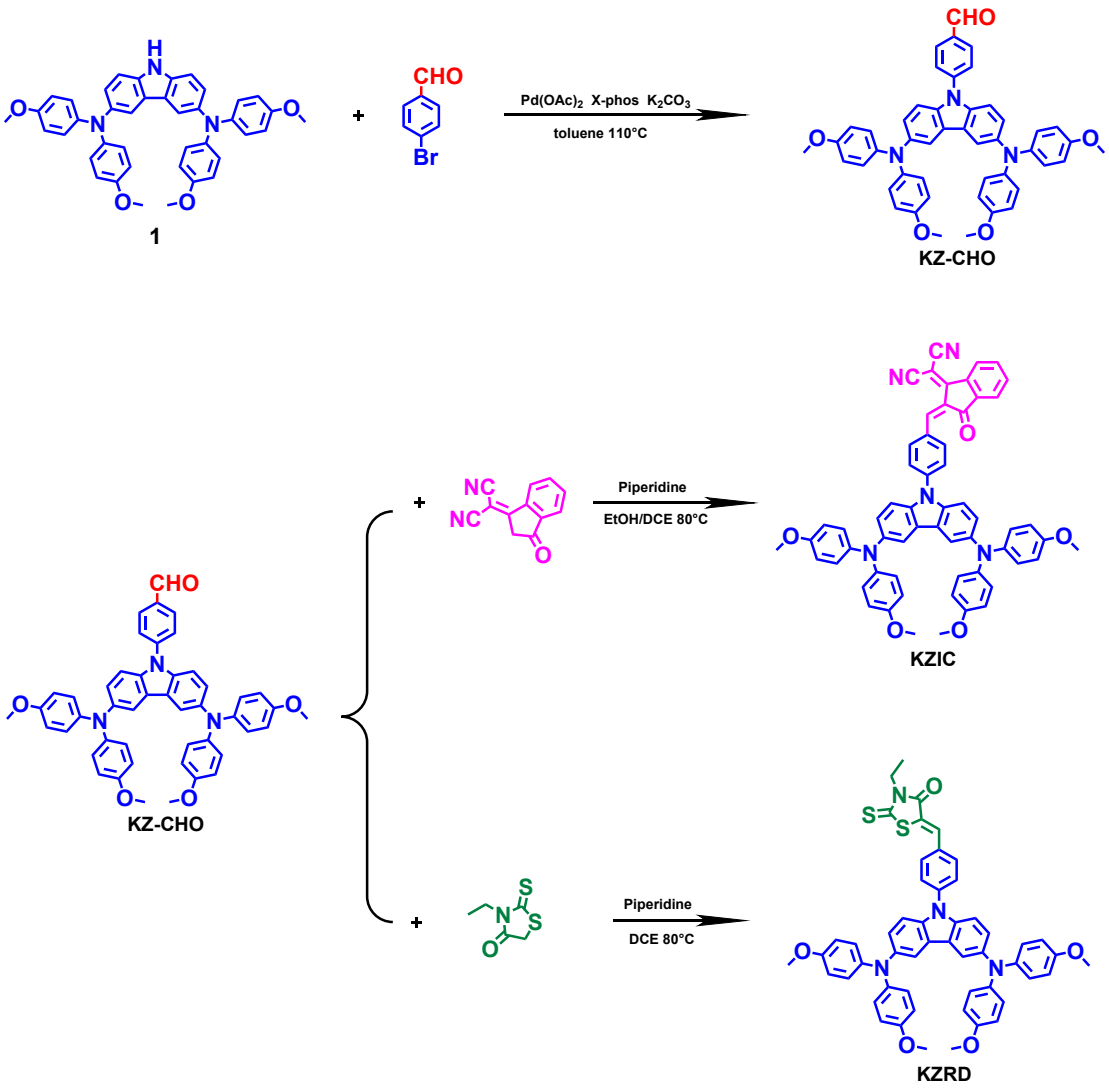

Scheme S1. Synthetic procedures for KZIC and KZRD.

Synthesis routes for KZIC and KZRD

KZ and the intermediate compound 1 were synthesized according to method reported in literature.[2]

Synthesis of KZ-CHO

A mixture of Compound 1 (50 mg, 0.08 mmol), 4-bromobenzaldehyde (22 mg, 0.12 mmol), $Pd(OAc)_2$ (1 mg, 0.0044 mmol), X-phos (4 mg, 0.0084 mmol) and K_2CO_3 solution (0.1 mL, 2 M in H_2O) in 5 ml toluene was heated at 110 °C for overnight under argon atmosphere. After cooling to room temperature, the reaction mixture was quenched with water and extracted with dichloromethane. Combined organic layers were dried over anhydrous Na_2SO_4 and concentrated

under vacuum to get crude residue which was purified by column chromatography using dichloromethane/hexane = 1:1 as the eluent to afford KZ-CHO as an orange powder (52 mg, 90%).^{1}H NMR (600 MHz, THF-d_8) δ 9.95 (s, 1H), 8.02 (d, J = 7.8 Hz, 2H), 7.73 (d, J = 7.8 Hz, 2H), 7.57 (s, 2H), 7.28 (d, J = 8.4 Hz, 2H), 6.99 (d, J = 8.4 Hz, 2H), 6.82 (d, J = 7.2 Hz, 8H), 6.64 (d, J = 9 Hz, 8H), 3.60 (s, 12H). ^{13}C NMR (150 MHz, $CDCl_3$) δ 190.80, 154.95, 142.65, 142.36, 136.59, 134.35, 131.36, 126.30, 124.77, 124.68, 124.19, 121.60, 116.13, 114.65, 110.57, 55.53.

Synthesis of KZIC

A mixture of KZ-CHO (300 mg, 0.41 mmol), 1-(dicyanomethylene)-3-indanone (460 mg, 2.37 mmol) and 1 ml piperdine in 20 ml EtOH :1,2-dichloroethane =1:1 was heated at 80 ^{o}C for overnight under argon atmosphere. After cooling to room temperature, the reaction mixture was quenched with water and extracted with dichloromethane. Combined organic layers were dried over anhydrous Na_2SO_4 and concentrated under vacuum to get crude residue which was purified by column chromatography using dichloromethane/ethyl acetate = 100:1 as the eluent to afford KZIC as a dark purple powder (129 mg, 35%).^{1}H NMR (600 MHz, $CDCl_3$) δ 7.86 (d, J = 7.2 Hz, 1H), 7.61 (s, 2H), 7.55-7.51 (m, 4H), 7.36-7.31 (m, 2H), 7.23. (d, J = 9 Hz, 2H), 7.08-7.06 (m, 2H), 6.97 (d, J = 8.4 Hz, 8H), 6.75 (d, J = 9 Hz, 8H), 5.81-5.78 (m, 2H), 3.76 (s, 12H). ^{13}C NMR (150 MHz, $CDCl_3$) δ189.54, 160.81, 154.70, 142.51, 141.81, 140.82, 139.33, 137.69, 137.41, 134.89, 131.85, 129.80, 127.59, 127.02, 124.39, 124.04, 121.18, 120.74, 119.70, 116.48, 114.57, 111.52, 110.55, 61.84, 55.53. MS for $C_{59}H_{43}N_5O_5$ m/z: $[M+H]^+$ calcd for 902.02; found 902.33.

Synthesis of KZRD

A mixture of KZ-CHO (300 mg, 0.41 mmol), 3-ethylrhodanine (121 mg, 0.82 mmol) and 0.5 ml piperidine in 20 ml 1,2-dichloroethane was heated at 80 ^{o}C for overnight under argon atmosphere.

After cooling to room temperature, the reaction mixture was quenched with water and extracted with dichloromethane. Combined organic layers were dried over anhydrous Na_2SO_4 and concentrated under vacuum to get crude residue which was purified by column chromatography using dichloromethane/hexane = 1:1 as the eluent to afford KZRD as a dark purple powder (139 mg, 39%).^{1}H NMR (600 MHz, THF-d_8) δ 7.75-7.69 (m, 5H), 7.56 (s, 2H), 7.29 (d, J = 8.4Hz, 2H), 7.00 (d, J = 8.4 Hz, 2H), 6.82 (d, J = 8.4 Hz, 8H), 6.64 (d, J = 9 Hz, 8H), 4.09-4.06 (m, 2H), 3.60 (s, 12H), 1.18-1.14 (m, 3H). ^{13}C NMR (150 MHz, $CDCl_3$) δ 192.64, 167.59, 154.90, 142.53, 142.38, 140.09, 136.70, 132.12, 131.60, 131.55, 126.70, 124.64, 124.21, 123.42, 116.18, 114.63, 110.58, 55.53, 39.90, 12.26. MS for $C_{52}H_{44}N_4O_5S_2$ m/z: $[M]^+$ calcd for 868.28; found 868.27.

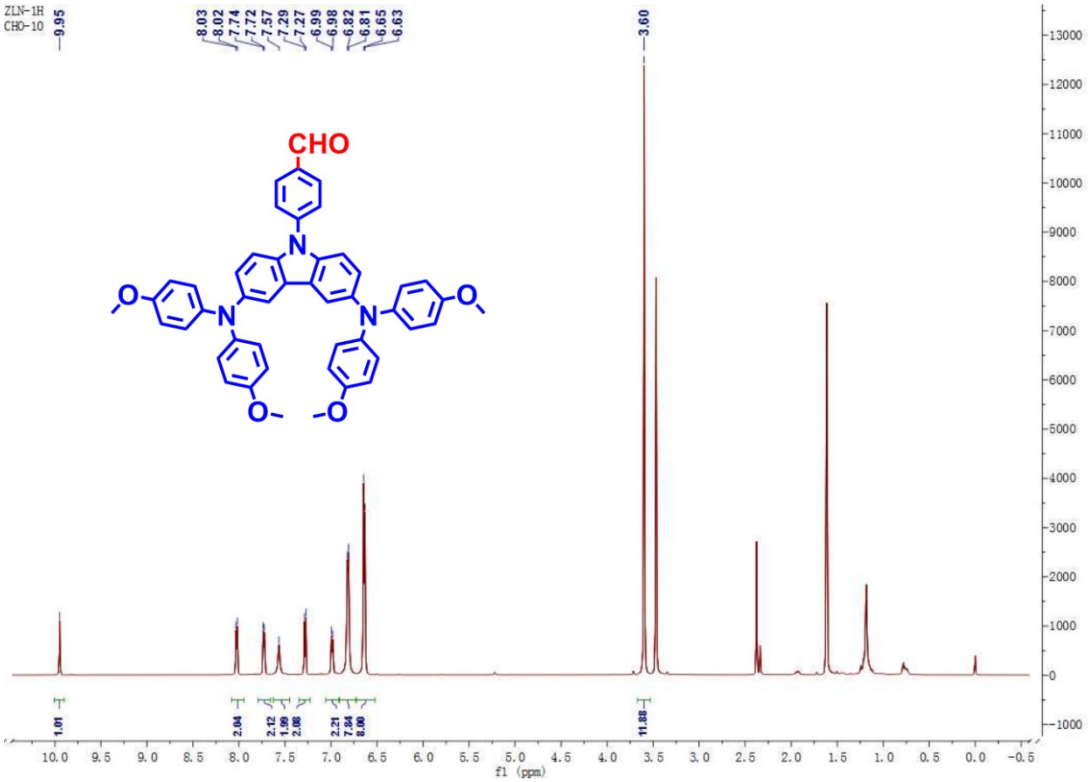

Figure S1. ^{1}HNMR of KZ-CHO.

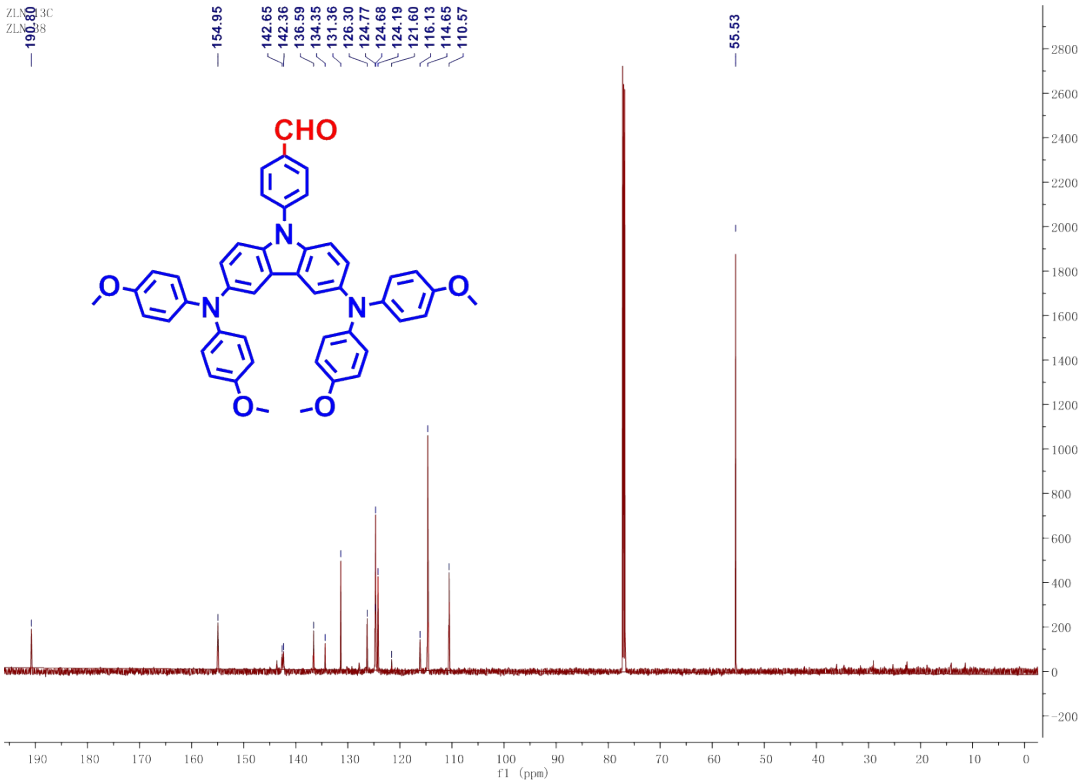

Figure S2. ^{13}CNMR of KZ-CHO.

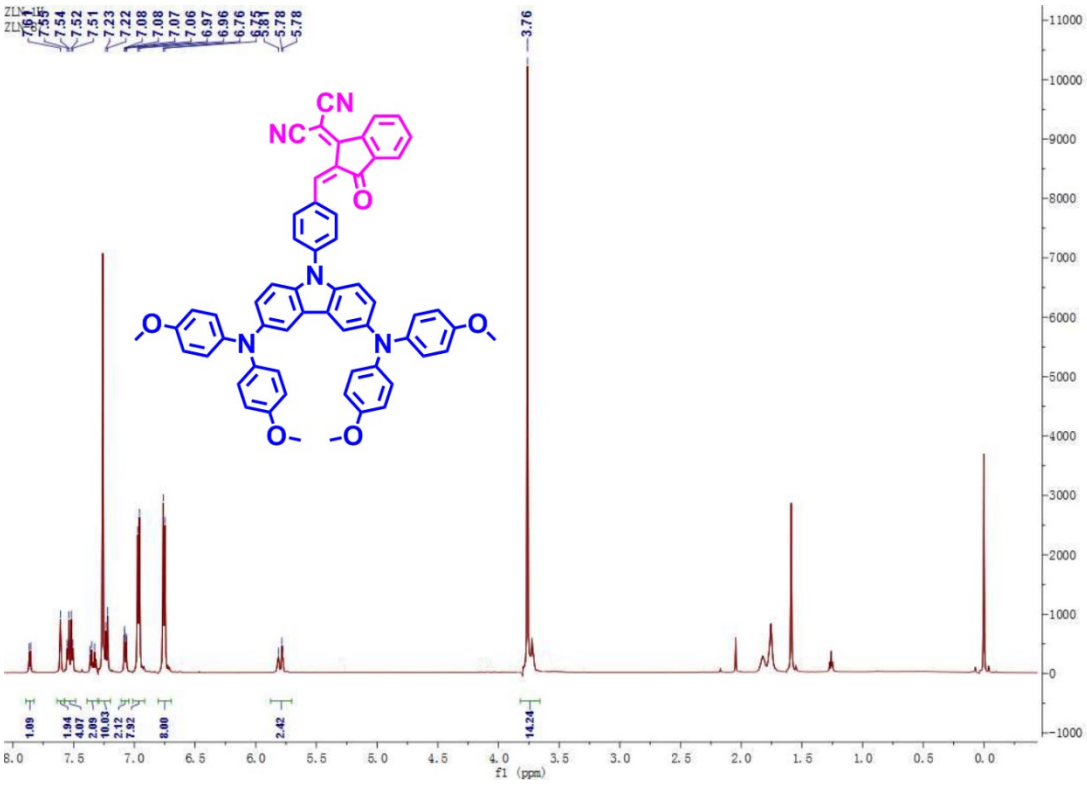

Figure S3. ^{1}HNMR of KZIC.

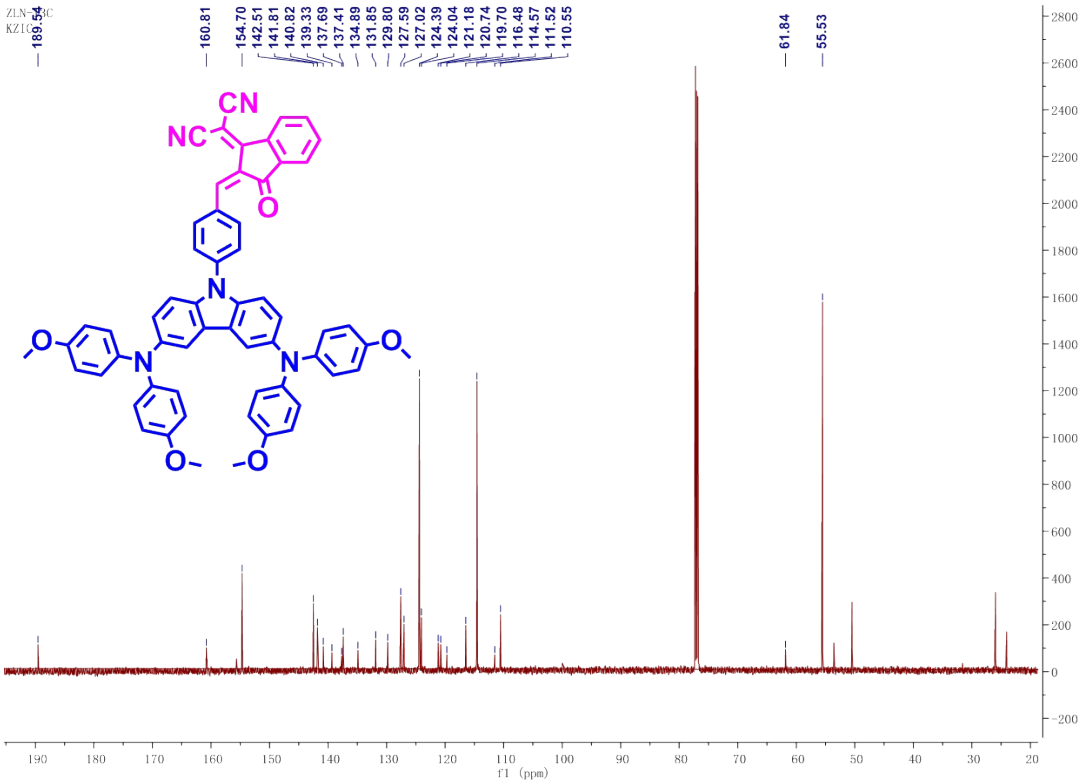

Figure S4. ^{13}CNMR of KZIC.

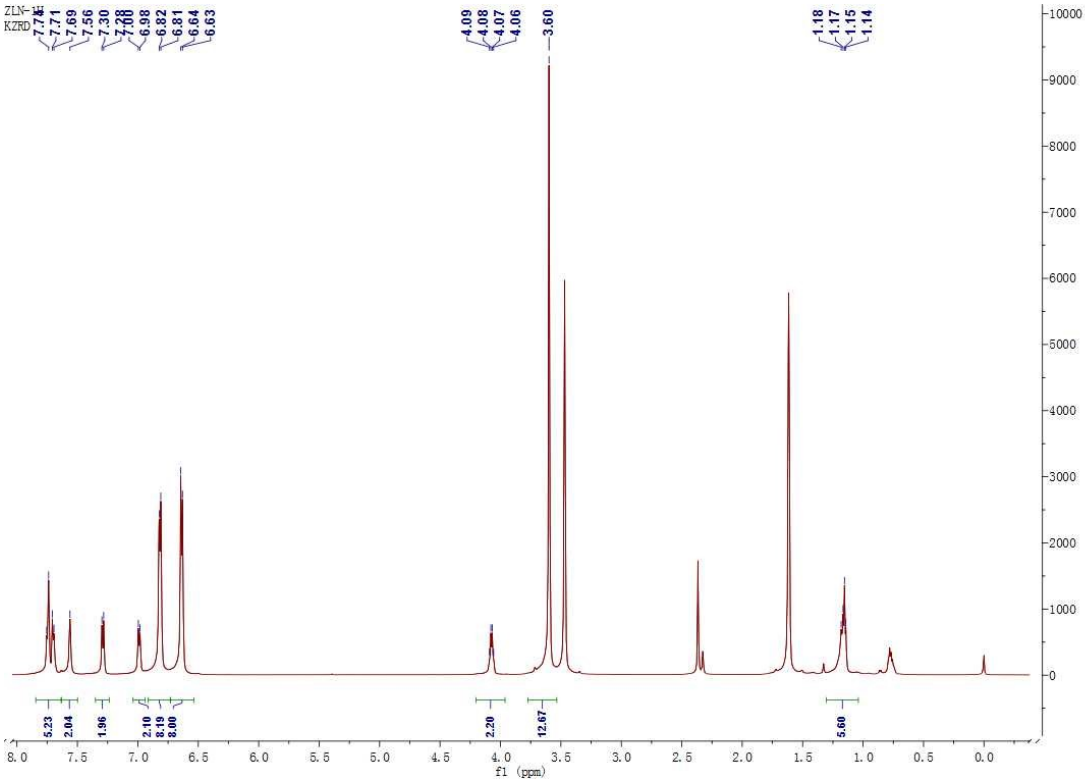

Figure S5. ^{1}HNMR of KZRD.

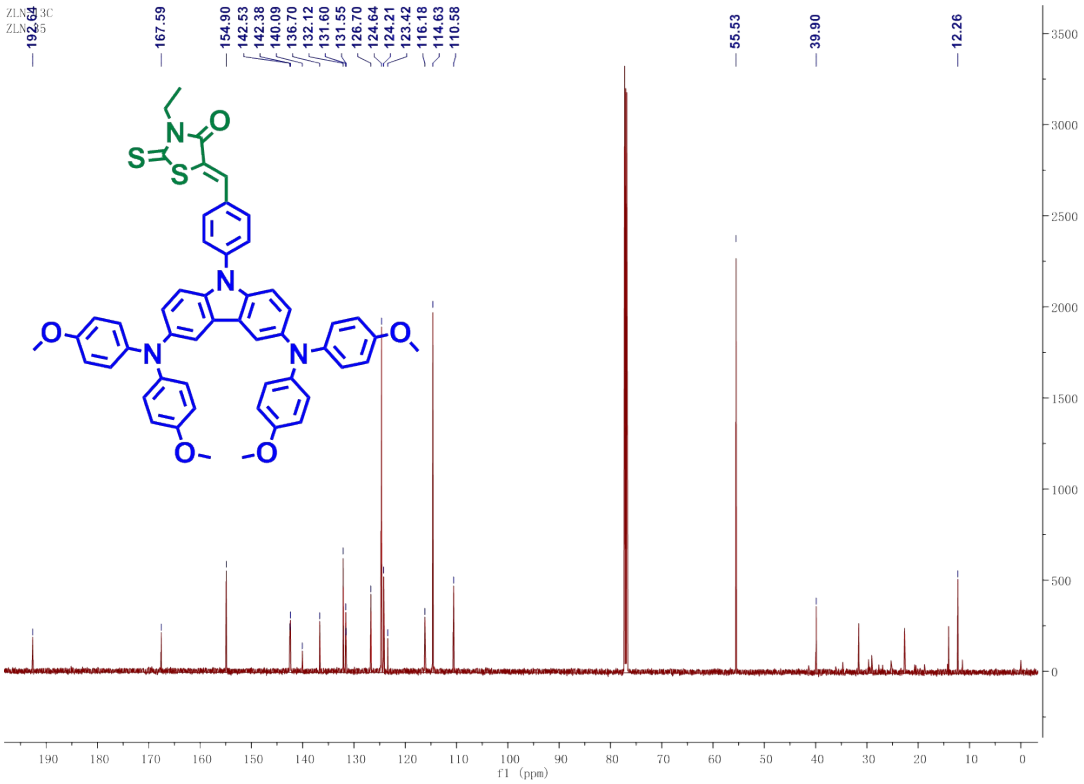

Figure S6. ^{13}CNMR of KZRD.

4. Electrical and photovoltaic properties

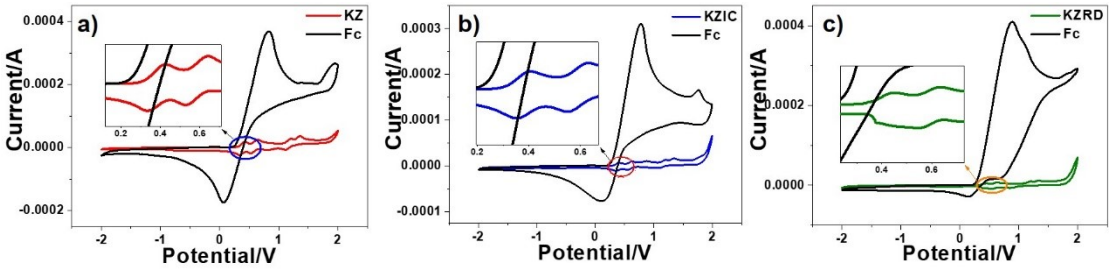

Figure S7. CV curves of KZ, KZIC and KZRD.

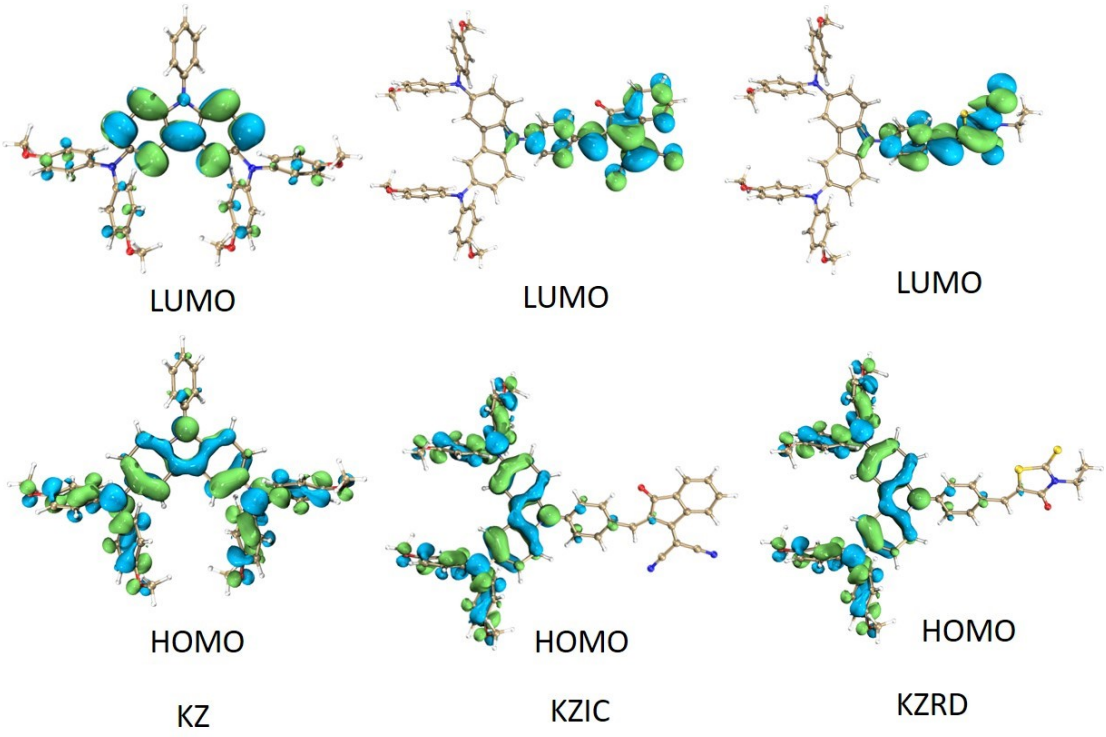

Figure S8. HOMO and LUMO orbital distributions and the optimized molecular structures of KZ, KZIC and KZRD.

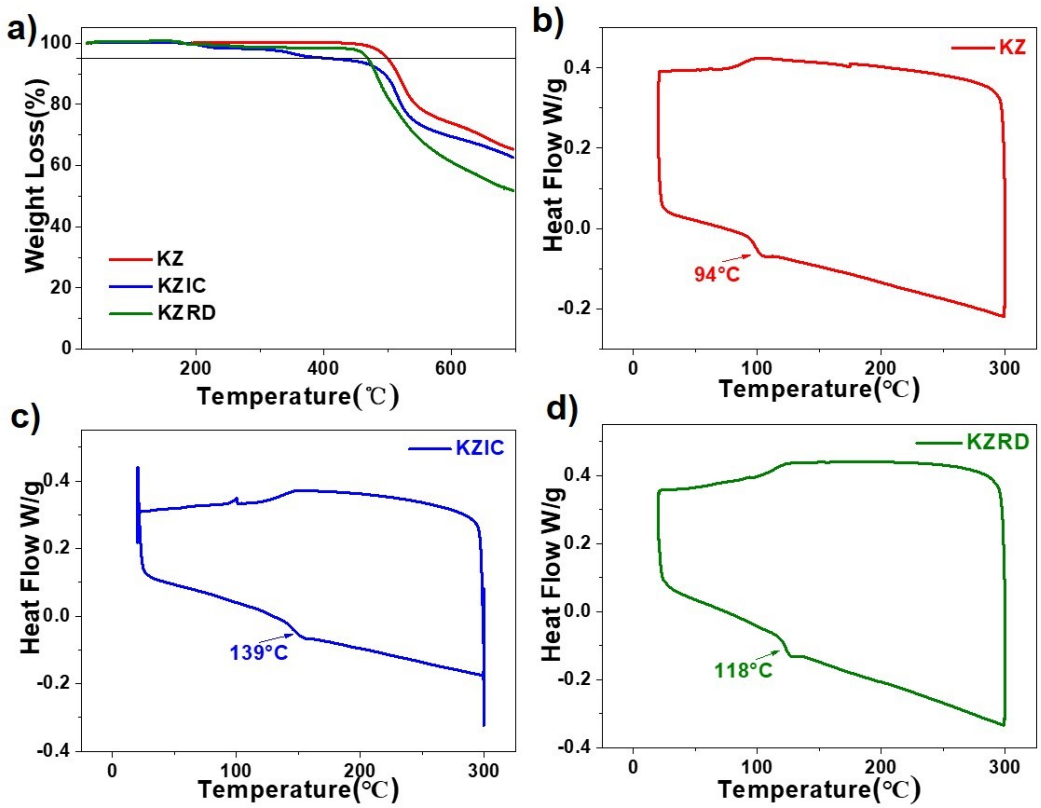

Figure S9. a) Thermogravimetric analysis (TGA) and b), c), d) Differential scanning calorimetry

(DSC) of KZ, KZIC and KZRD under N_2 atmosphere.

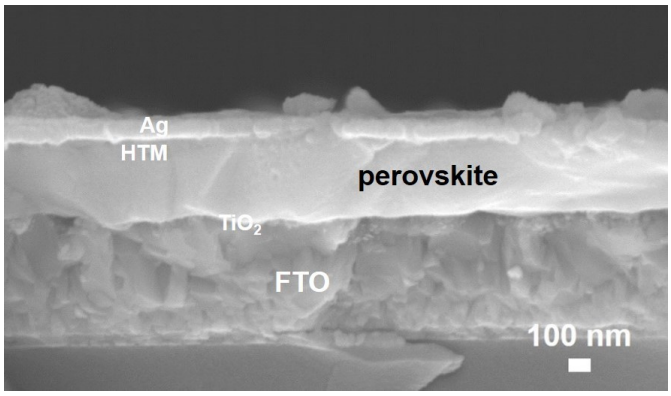

Figure S10. Cross-sectional SEM image of perovskite with KZRD as the HTM.

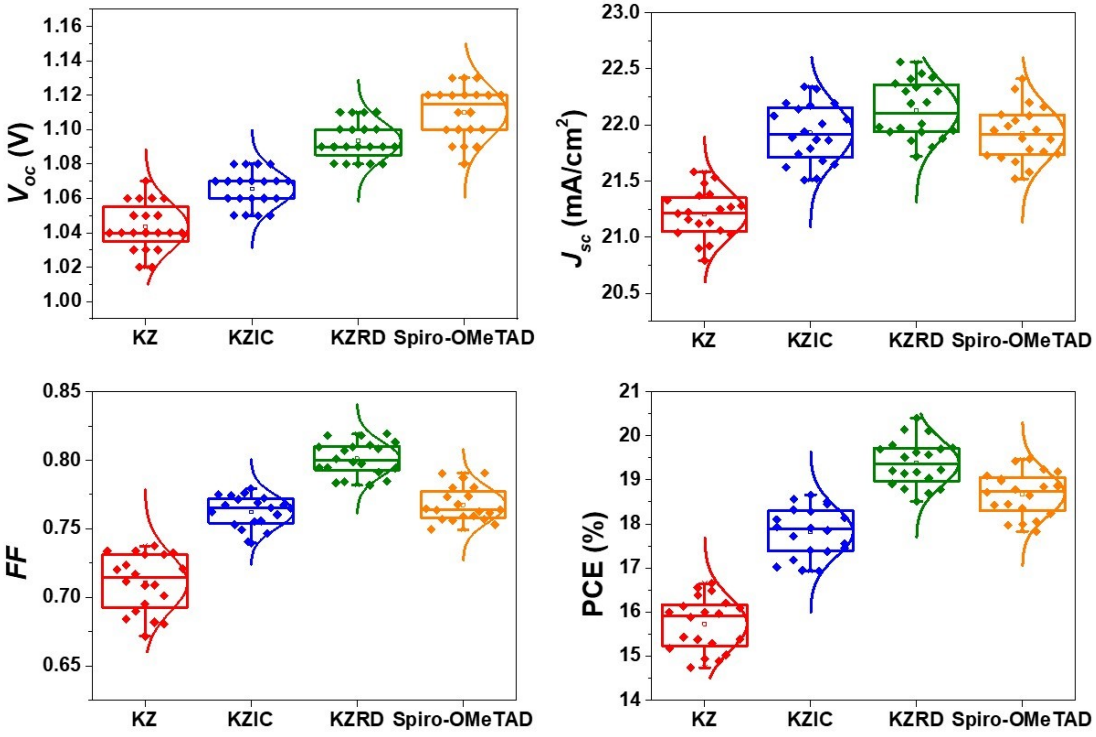

Figure S11. a) V_{oc}, b) J_{sc}, c) *FF*, and d) PCE statistics of 20 devices employing different HTMs.

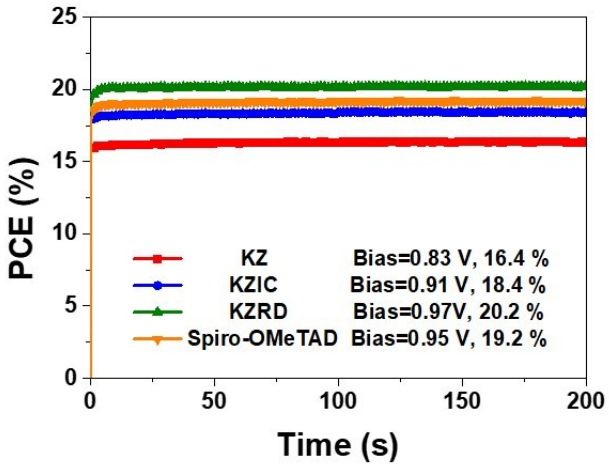

Figure S12. Stabilized PCE of PSCs with different HTMs.

Table S1. Photovoltaic parameters of forward and reverse scanning of PSCs with different HTMs.

Devices	V_{oc}**(V)**	J_{sc}**(mA/cm²)**	**FF**	**PCE(%)**
Spiro-OMeTAD forward	1.12	22.08	0.79	19.47
Spiro-OMeTAD reverse	1.08	22.05	0.74	17.61
KZ forward	1.06	21.48	0.73	16.65
KZ reverse	1.04	21.48	0.65	14.44
KZIC forward	1.08	22.17	0.78	18.66
KZIC reverse	1.07	22.14	0.75	17.75
KZRD forward	1.11	22.46	0.82	20.40
KZRD reverse	1.10	22.42	0.78	19.20

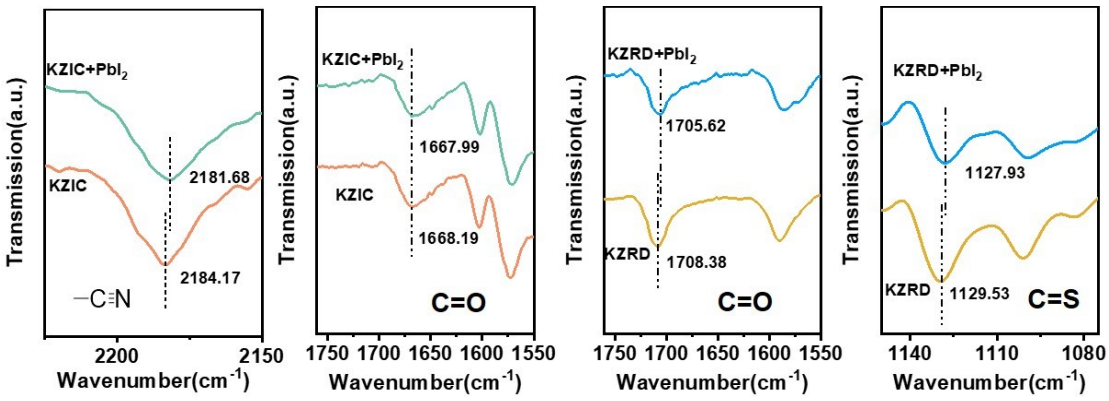

Figure S13. Characteristic FTIR spectra changes of KZIC and KZRD with and without PbI_2.

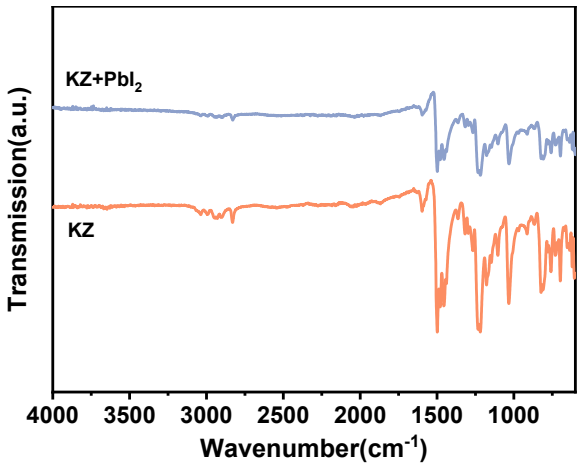

Figure S14. FTIR spectra of KZ with and without PbI_2.

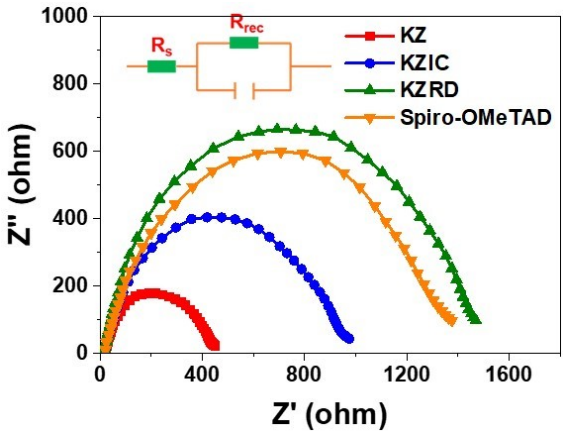

Figure S15. Nyquist plots of PSCs based on different HTMs. The inset shows the equivalent circuit

model.

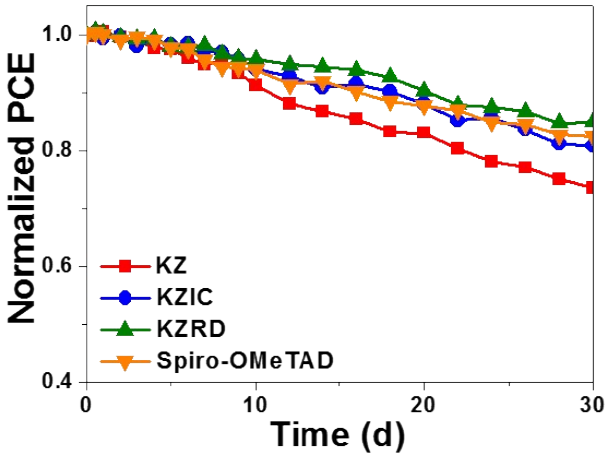

Figure S16. Stability tests of the PSCs with different HTMs in a N_2-filled glovebox without encapsulation.

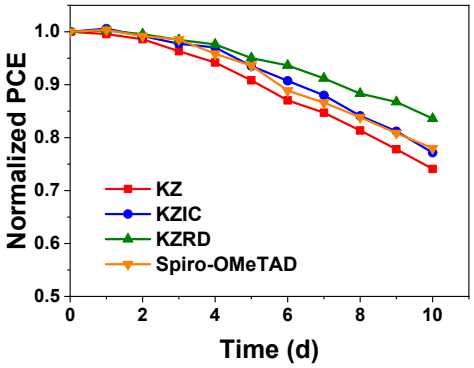

Fig. S17 Stability tests of perovskite solar cells using different HTMs measured in ambient conditions. (The devices were stored in ambient condition, with the room temperature at about 26°C, and air humidity of 30-35 %.)

References:

[1] Y. Ji, B. He, H. Lu, J. Xu, R. Wang, Y. Jin, C. Zhong, Y. Shan, F. Wu and L. Zhu, 2019, 12, 1374-1380.

[2] M. Li, Z. Wang, M. Liang, L. Liu, X. Wang, Z. Sun and S. Xue, The Journal of Physical Chemistry C, 2018, 122, 24014-24024.